Computer Methods in Biomechanics and Biomedical Engineering, 2015
Vol. 18, No. 5, 506–513, http://dx.doi.org/10.1080/10255842.2013.818666

Muscle moment-arms: a key element in muscle-force estimation

David Ingram[a1], Christoph Engelhardt[b2], Alain Farron[c], Alexandre Terrier[b3] and Philippe Müllhaupt[a]*

[a]*Labortatoire d'Automatique, Ecole Polytechnique Fédérale de Lausanne, Station 9, 1015 Lausanne, Switzerland;*
[b]*Laboratory of Biomechanical Orthopedics, Ecole Polytechnique Fédérale de Lausanne, Station 19, 1015 Lausanne, Switzerland;*
[c]*Service of Orthopaedics and Traumatology, University Hospital Centre, University of Lausanne, Rue du Bugnon 46, 1011 Lausanne, Switzerland*

(*Received 9 January 2013; accepted 19 June 2013*)

A clear and rigorous definition of muscle moment-arms in the context of musculoskeletal systems modelling is presented, using classical mechanics and screw theory. The definition provides an alternative to the tendon excursion method, which can lead to incorrect moment-arms if used inappropriately due to its dependency on the choice of joint coordinates. The definition of moment-arms, and the presented construction method, apply to musculoskeletal models in which the bones are modelled as rigid bodies, the joints are modelled as ideal mechanical joints and the muscles are modelled as massless, frictionless cables wrapping over the bony protrusions, approximated using geometric surfaces. In this context, the definition is independent of any coordinate choice. It is then used to solve a muscle-force estimation problem for a simple 2D conceptual model and compared with an incorrect application of the tendon excursion method. The relative errors between the two solutions vary between 0% and 100%.

Keywords: musculoskeletal systems; moment-arms; screw theory; muscle-force estimation

1. Introduction

Musculoskeletal systems such as the shoulder, the hip or the knee are largely modelled as a set of rigid bodies, representing the bones, connected together by ideal mechanical joints, representing the anatomical joints. The muscles are modelled as massless, frictionless cables wrapping over the bones from origin to insertion, with a uniform tension throughout the cable. The bones and joints define the system and the muscles act as external force generators on the system. Therefore, such models fall into the domain of classical mechanics and are governed by Newton's laws of motion.

In Newton's second law, the link between the force generated by a muscle and the motion of the system is the muscle moment-arm. Muscle moment-arms were initially defined experimentally in cadaveric studies, by relating the change in muscle length to the change in joint angle (Brand et al. 1975; An et al. 1983; Otis et al. 1994; Liu et al. 1997; Ackland et al. 2008). This experimental definition was formalised using the principle of virtual work, leading to the tendon excursion definition, by which the moment-arm is defined as partial derivative of the muscle length with respect to the joint angle (An et al. 1984).

Because of its simplicity and relation to the experimental definition, the tendon excursion method has been widely used to compute and validate model-based moment-arms (Charlton and Johnson 2001; Garner and Pandy 2001; Holzbaur et al. 2005). However, it is a definition which requires caution and a certain amount of rigour. Because the tendon excursion method is defined using the principle of virtual work, a concept from analytical mechanics, it must be applied according to the same framework, and using the same hypothesis. Thus, the coordinates used to construct the definition are not just any joint coordinates, but the generalised coordinates used to describe the musculoskeletal model. This last point is key: the tendon excursion method is dependent on the choice of generalised coordinates and must be used accordingly.

The tendon excursion method has, however, been used without rigorous justification in a number of cases from the literature (Herzog and Binding 1992; Raikova and Prilutsky 2001; Menegaldo et al. 2004; Rankin and Neptune 2012). This has led to the definition that muscles define moment-arms only at the joints spanned by the muscle. A more rigorous application of the method finds moment-arms at the joints spanned by the muscle *and* at the joints attached to the bodies on which the muscles insert and originate. The moment-arms which are omitted have a coupling effect between the muscles. In the muscle-force estimation problem as defined by Happee (1994), the omission of the coupling effect leads to a relaxation of the optimisation problem and ultimately a different solution. This change in solution can also have effects on the joint

*Corresponding author. Email: philippe.muellhaupt@epfl.ch

reaction forces. In contrast, if the coupling moment-arms are not omitted, the estimation problem, can in certain cases, be infeasible. A point observed in Ingram et al. (2012), where a musculoskeletal shoulder model is presented.

The goal of this paper is to present a rigorous, clear and unambiguous definition of muscle moment-arm, using screw theory. The definition is independent of the choice of coordinates, and yields a systematic method of computing muscle moment-arms. The effect of considering the coupling terms or not is assessed by solving a muscle-force estimation problem using a conceptual 2D musculoskeletal model similar to the that presented in Herzog and Binding (1992). The estimation problem is solved using inverse dynamics and static optimisation. The optimisation problem is solved using a geometric method which computes an initial solution using a pseudo-inverse of the moment-arm matrix defining the moment of force/muscle-force map. The initial solution is modified by parameterising the final solution in terms of the matrix null-space. The results are analysed in terms of the estimated muscle forces and the joint reaction forces. Two calculations of moment-arms are compared: (1) total moment-arms and (2) approximation without coupling moment-arms.

2. Methods

2.1 A definition of muscle moment-arm

In classical mechanics, a force $\mathbf{f}$, applied on a rigid body $\mathscr{B}$ at point A, creates a moment of force at any other point B of the body (Figure 1). The moment of force $\mathbf{t}$ is defined as the cross product between the vector $\mathbf{r}$ from points B to A and the force.[4] The force and its moment, if grouped together in an ordered pair, define a screw or wrench with respect to point B in this case (Ball 1876; Whittaker 1927; Gruber and Benoit 1998):

$$\mathbf{S}_{\mathrm{B}} = (\mathbf{f},\, \mathbf{r}\times\mathbf{f})_{\mathrm{B}} = |f|(\mathbf{d},\, \mathbf{r}\times\mathbf{d})_{\mathrm{B}} = |f|(\mathbf{d},\, \mathbf{m})_{\mathrm{B}}. \quad (1)$$

The associated moment-arm $\mathbf{m}$ is defined by the same cross product but with a normalised force vector $\mathbf{d}$. This definition of moment-arm applies to a single body subject to a single force, and has a geometric interpretation. The norm of the moment-arm represents the distance from point B to the line defined by vector $\mathbf{d}$ passing through A, a quantity called the lever-arm. The moment-arm is, therefore, a purely geometric quantity associated with a given point on the body, which depends only on the direction of the force and its point of application.

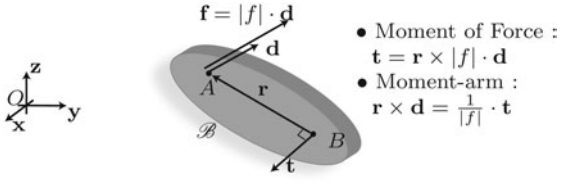

Figure 1. Diagram of the classical mechanics definition of muscle moment-arm.

There is another interpretation of the moment-arm. If the body is attached to a fixed point through a spherical joint at the point B, and no other force is applied to the body, then the moment-arm vector defines the instantaneous axis of rotation of the body around the joint.

As stated in the introduction, a musculoskeletal system is defined by a number of bones and joints, while the muscles act as external force generators. In terms of classical mechanics, there are multiple bodies $\mathscr{B}_i$ connected by multiple joints J_i. Each muscle is modelled as a massless, frictionless cable. Pulley mechanics are used to compute the points of application and direction of the forces applied by the muscles on the bodies. Accordingly, a cable applies a force at the first point of attachment, parallel to the cable and pointing along the cable, and a second force at the second point of attachment, parallel to the cable and pointing along the cable. If the muscle wraps over a bone, it applies two forces on the bone at the initial and final points of contact which are pointing in opposite directions parallel to the cable and of same magnitude. According to this description, a muscle applies multiple forces $\mathbf{f}_k$ to the bodies and creates moment-arms for every body to which it applies a force. The moment-arm of a force is defined with respect to a specific point B on the body. Thus, muscle moment-arms are also defined with respect to a specific point, usually one of the joints attached to the body.

For a specific muscle, the moment-arms on each body are computed by isolating each body and considering the forces applied by the muscle on the body, keeping in mind that forces are transmitted through the joints. The total moment-arm is then defined as the sum of the moment-arms created by each force $\mathbf{f}_k$ at one of the joints J_i associated with the body

$$S_{J_i} = \sum_{k=1}^{m} \left(\mathbf{f}_k, \mathbf{r}_k\times\mathbf{f}_k\right) = |f|\sum_{k=1}^{m} \left(\mathbf{d}_k, \mathbf{r}_k\times\mathbf{d}_k\right). \quad (2)$$

The total moment-arm is obtained by dividing the total moment-force by the norm of the force

$$\mathbf{m}_{J_i} = \frac{1}{|f|}\sum_{k=1}^{m} \mathbf{r}_k\times\mathbf{f}_k = \sum_{k=1}^{m} \mathbf{r}_k\times\mathbf{d}_k. \quad (3)$$

Thus, by proceeding systematically, the moment-arm around each joint is calculated exactly.

To illustrate the definition, consider the conceptual 2D musculoskeletal system represented in Figure 2, similar to the model from Herzog and Binding (1992). The model includes 10 muscles. Two muscles, $\mathscr{M}_1$ and $\mathscr{M}_2$ span the first joint. Another two muscles, $\mathscr{M}_5$ and $\mathscr{M}_6$ span the

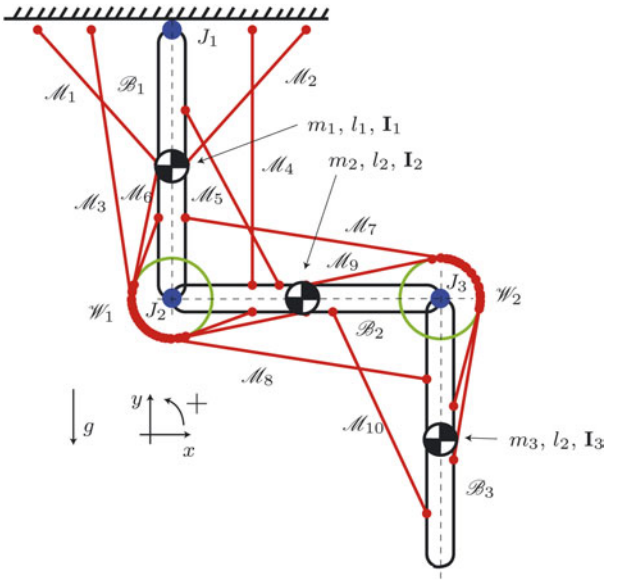

Figure 2. Diagram of a conceptual 2D musculoskeletal system.

second joint. A third pair of muscles $\mathscr{M}_9$ and $\mathscr{M}_{10}$ spans the third joint. A pair of muscles $\mathscr{M}_3$ and $\mathscr{M}_4$ spans both the first and second joints while the last pair of muscles $\mathscr{M}_7$ and $\mathscr{M}_8$ spans the second and third joints. The muscles wrap around two bony protrusions modelled as circles: $\mathscr{W}_1$ and $\mathscr{W}_2$. Centred at the second and third joints, respectively, $\mathscr{W}_1$ is attached to the first bone while $\mathscr{W}_2$ is attached to the second bone. This point is important because it gives a particular set of moment-arms following the previously stated definition. If the wrappings were changed by associating $\mathscr{W}_1$ with the second bone and $\mathscr{W}_2$ with the third, the moment-arms would be different.

The moment-arms of muscle $\mathscr{M}_8$ around the joints are computed explicitly by isolating each body with the forces applied by the muscle (Figure 3). Starting with the distal body $\mathscr{B}_3$, the muscle applies a force $\mathbf{f}_2$ at point P_4. This force is transmitted through the third joint J_3 to the second body $\mathscr{B}_2$. The force is transmitted again through the second joint J_2 to the first body $\mathscr{B}_1$. The muscle also applies a force $-\mathbf{f}_2$ directly on the first body at P_3 and two equal and opposite forces $\mathbf{f}_1$ and $-\mathbf{f}_1$ at P_1 and P_2, which cancel each other. All the forces have the same norm $|f_8|$.

The muscle moment-arm at the third joint J_3 is defined by

$$S_{J_3} = \left(\mathbf{f}_2,\ \vec{J_3P_4} \times \mathbf{f}_2\right) \Rightarrow \mathbf{m}_{J_3} = \frac{1}{|f_8|}\left(\vec{J_3P_4} \times \mathbf{f}_2\right). \quad (4)$$

The muscle moment-arm at the second joint J_2 is defined by

$$S_{J_2} = \left(\mathbf{f}_2,\ \vec{J_2J_3} \times \mathbf{f}_2\right) \Rightarrow \mathbf{m}_{J_2} = \frac{1}{|f_8|}\left(\vec{J_2J_3} \times \mathbf{f}_2\right). \quad (5)$$

The muscle moment-arm at the first joint J_1 is defined by

$$\begin{aligned} S_{J_1} &= \left(\mathbf{f}_2, \vec{J_1J_2} \times \mathbf{f}_2\right) - \left(\mathbf{f}_2, \vec{J_1P_3} \times \mathbf{f}_2\right) \\ &= \left(0,\ \left(\vec{J_1J_2} - \vec{J_1P_3}\right) \times \mathbf{f}_2\right), \\ \Rightarrow \mathbf{m}_{J_1} &= \frac{1}{|f_8|}\left(\vec{J_1J_2} - \vec{J_1P_3}\right) \times \mathbf{f}_2. \end{aligned} \quad (6)$$

Muscle $\mathscr{M}_8$ does not span the first joint J_1, but it does create a moment-arm around this joint. The moment-arms for the other muscles are computed in a similar manner. It should be noted that while the muscle creates a moment-arm at the joint which it does not span, it does not, however, create a force. The resulting forces of the muscle at the joints not spanned by the muscle are always zero. This point provides a means of verifying the application of the definition.

To demonstrate the result of non-zero moment-arms around joints not spanned by the muscle using the tendon excursion method, a coordinate θ_i is associated with each joint representing the absolute angle with respect to the absolute y-axis (Figure 4). The configuration of the system in Figure 2 is defined as the initial configuration. In this

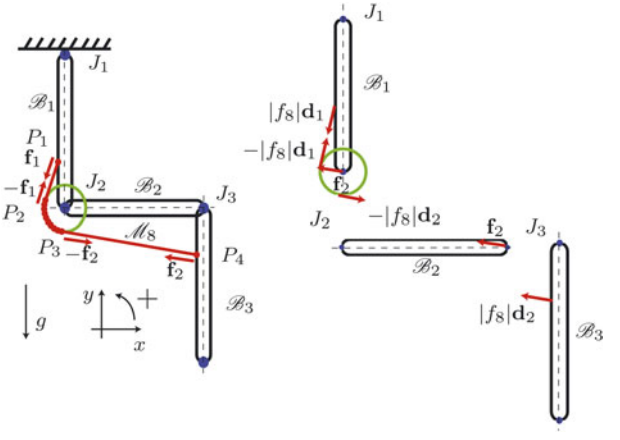

Figure 3. Diagram of the forces applied by muscle $\mathscr{M}_8$ on the different bodies.

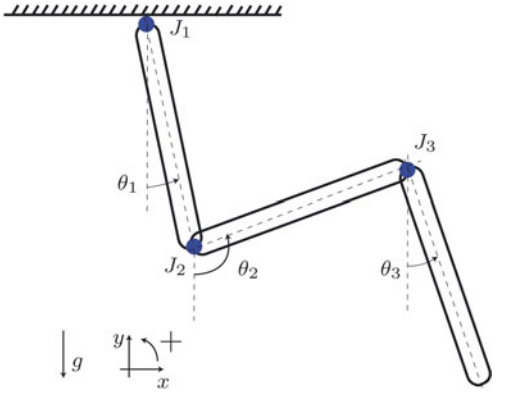

Figure 4. Diagram of the joint coordinate definitions.

configuration, the length of muscle $\mathscr{M}_8$ is defined as

$$L_8 = \left\| \vec{J_2P_2} - \vec{J_2P_1} \right\|_2 + \left\| \vec{J_2P_4} - \vec{J_2P_3} \right\|_2 + d(P_2, P_3), \quad (7)$$

where $\|\cdot\|_2$ is the Euclidean norm and $d(P_2, P_3)$ is the length of the circular arc between the wrapping contact points P_2 and P_3:

$$d(P_2, P_3) = \left| R \arccos\left(1 - \frac{\left\| \vec{J_2P_3} - \vec{J_2P_2} \right\|_2^2}{2R^2} \right) \right|, \quad (8)$$
$$R = \left\| \vec{J_2P_2} \right\|_2 = \left\| \vec{J_2P_3} \right\|_2,$$

as defined in Garner and Pandy (1999).

The angle of the first joint is then changed by $\Delta\theta_1$, while leaving the other two joints in their initial configuration (Figure 5). The new configuration is superimposed to the initial configuration and the origin O of both configurations is set at the centre of the second joint J_2 (Figure 5). With respect to this reference system points P_3 and P_4 remain unchanged. Because the distance between the origin of muscle P_1 and the centre of the second joint has not changed, the triangles $\Delta P_1 J_2 P_2$ and $\Delta P'_1 J_2 P'_2$ are equivalent but rotated with respect to one another (Figure 5). Therefore, the distances (P_1, P_2) and (P'_1, P'_2) are the same. However, the arc lengths P_2, P_3 and P'_2, P'_3 are different because the wrapping point $P_2 \neq P'_2$ while $P_3 = P'_3$. Thus, the muscle length has changed and is now defined by

$$\begin{aligned} L'_8 &= \left\| \vec{J_2P'_2} - \vec{J_2P'_1} \right\|_2 + \left\| \vec{J_2P'_4} - \vec{J_2P'_3} \right\|_2 + d\left(P'_2, P'_3\right) \\ &= L_8 + d\left(P'_2, P'_3\right) - d(P_2, P_3). \end{aligned} \quad (9)$$

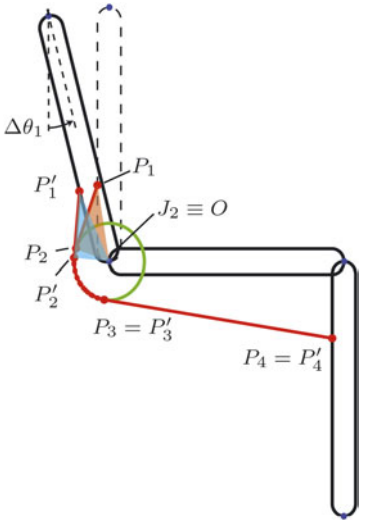

Figure 5. (Colour online) Diagram of the superimposed configurations. The equivalent triangles are in orange and blue.

Applying the tendon excursion method to the previous result leads to the moment-arm around the first joint

$$\mathbf{m}_{J_1} = \lim_{\Delta\theta_1 \to 0} -\frac{L'_8 - L_8}{\Delta\theta_1} = \lim_{\Delta\theta_1 \to 0} -\frac{d\left(P'_2, P'_3\right) - d\left(P_2, P_3\right)}{\Delta\theta_1} \neq 0. \quad (10)$$

With a bit of mathematical development (not presented here), this limit is shown to be non-zero as will be illustrated in the following section.

2.2 A muscle-force estimation problem

The bones of the musculoskeletal system (Figure 2) are given masses m_i, lengths l_i and inertia tensors $\mathbf{I}_i$. The centre of gravity of each bone is located at the mid point, and the system is such that the y-axis is aligned with the direction of gravity. The mass, length and inertia of each bone are defined as 1 (kg), (m) and (kg m^2).

Using the coordinates defined previously and their derivatives and choosing the positive rotation as counter-clockwise, a dynamic model is defined (Yeung 1995). The model is of the form

$$\mathbf{x} = \begin{pmatrix} \theta_1 & \theta_2 & \theta_3 \end{pmatrix}^{\mathrm{T}}, \quad z = \dot{\mathbf{x}}, \quad (11)$$

$$\mathbf{M}(\mathbf{x})\dot{\mathbf{z}} = \mathbf{h}(\mathbf{x}, \mathbf{z}) + \mathbf{t}, \quad (12)$$

where $\mathbf{M}(\mathbf{x})$ is the dynamic inertia matrix, $\mathbf{h}(\mathbf{x}, \mathbf{z})$ contains the internal dynamics due to gravity, coriolis, etc. Vector $\mathbf{t}$ is the moment of force applied by the muscles. The muscle forces $\mathbf{f}$ are linked to the torque vector through the moment-arms, which are grouped into a matrix leading to the relation

$$\mathbf{t} = \mathbf{W}(\mathbf{x}) \cdot \mathbf{f}. \quad (13)$$

The moment-arm matrix $\mathbf{W}(\mathbf{x})$ is dependent on the configuration $\mathbf{x}$. Using the approach described in the previous section, the moment-arm matrix has the following structure:

$$\mathbf{W}(\mathbf{x}) = \begin{pmatrix} w_{1,1} & w_{1,2} & w_{1,3} & w_{1,4} & w_{1,5} & w_{1,6} & w_{1,7} & w_{1,8} & 0 & 0 \\ 0 & 0 & w_{2,3} & w_{2,4} & w_{2,5} & w_{2,6} & w_{2,7} & w_{2,8} & w_{2,9} & w_{2,10} \\ 0 & 0 & 0 & 0 & 0 & 0 & w_{3,7} & w_{3,8} & w_{3,9} & w_{3,10} \end{pmatrix}. \quad (14)$$

where $w_{i,j}$ are the moment-arms of muscle j around joint i. Thus, the torque–force relation defines a locally linear map. For each static configuration the map is linear, but the dependency on the configuration is nonlinear.

To illustrate the point that the tendon excursion method and the presented definition yield identical moment-arms, the moment-arms are computed for all the

Table 1. Position (x, y) of muscle origin and insertion points in initial configuration.

Muscle ID	1	2	3	4	5
Origin	(−0.5, 0)	(0.5, 0)	(−0.3, 0)	(0.3, 0)	(0.05, −0.3)
Insertion	(−0.05, −0.5)	(0.05, −0.5)	(0.3, −1.05)	(0.3, −0.95)	(0.4, −0.95)
Muscle ID	6	7	8	9	10
Origin	(−0.05, −0.5)	(−0.05, −0.7)	(0.05, −0.7)	(0.5, −0.95)	(0.6, −1.05)
Insertion	(0.5, −1.05)	(0.95, −1.3)	(1.05, −1.4)	(1.05, −1.8)	(0.95, −1.8)

Note: Data in m.

muscles in the initial configuration using both methods. The tendon excursion method is applied using $\Delta\theta_i = 10^{-6}$. The position of the muscle origin and insertion points is given in Table 1 for the initial configuration. The bones are all considered of length 1 m. The radius of the wrapping circles is taken as $r = 0.15$ m. The absolute value of the relative error between the moment-arms is given by the matrix

$$\mathrm{Err}_{\mathrm{Rel}} = 10^{-3}.$$

$$\begin{pmatrix} 2.27 & 2.26 & 1.45 & 0 & 1.56 & 0 & 0.01 & 0.05 & 0 & 0 \\ 0.01 & 0.88 & 1.56 & 0.01 & 0.12 & 0.09 & 0 & 1.37 & & \\ 0 & 0 & 0 & 0 & 0 & 0 & 0.06 & 0.03 & 0 & 1.37 \end{pmatrix},$$

$$(\mathrm{Err}_{\mathrm{Rel}})_{ij} = \left| \frac{w_{i,j}^{\text{Tendon excursion method}} - w_{i,j}^{\text{Exact definition}}}{w_{i,j}^{\text{Exact definition}}} \right|.$$

Thus, the tendon excursion method and the presented definition yield identical moment-arms minus the numerical precision.

The muscle-force estimation problem is defined in this paper as the following problem. Given a dynamic motion of the system: $\mathbf{x}(t)$, $\mathbf{z}(t)$, $\dot{\mathbf{z}}(t)$ and the associated joint torques $\mathbf{t}(t)$, obtained through inverse dynamics, the muscle forces are estimated at any time t_k through a static optimisation problem. The cost function is defined as the mean square muscle stress. Muscle stress is defined as the force within the muscle divided by the physiological cross-section area (PCSA). The problem is also subject to lower and upper bounds on the muscle forces:

$$\min \quad g(\mathbf{f}_k) = \sum_{i=1}^{10} \left(\frac{(f_i)_k}{\mathrm{PCSA}_i} \right)^2, \tag{15}$$

$$\text{s.t.} \quad \mathbf{t}(t_k) = \mathbf{W}(\mathbf{x}(t_k)) \cdot \mathbf{f}_k, \quad \text{torque–force constraint}, \tag{16}$$

$$0 \leq \mathbf{f}_k \leq \mathbf{f}^{\max}, \quad \min/\max \text{ force}. \tag{17}$$

The optimisation problem is solved using a geometric method described subsequently. The maximum force and PCSA values are defined for all muscles in pairs of two (Table 2).

Table 2. Maximum force and PCSA values for all muscles.

Muscle ID	1, 2	3, 4	5, 6	7, 8	9, 10
$F_{\max}$ (N)	400	400	400	400	400
PCSA (cm^2)	0.5	0.7	4	0.1	4

For the model under consideration, the coupling terms are $w_{1,5}$, $w_{1,6}$, $w_{1,7}$, $w_{1,8}$, $w_{2,9}$ and $w_{2,10}$. Omitting these terms leads to the following moment-arm matrix:

$$\mathbf{W}(\mathbf{x}) = \begin{pmatrix} w_{1,1} & w_{1,2} & w_{1,3} & w_{1,4} & 0 & 0 & 0 & 0 & 0 & 0 \\ 0 & 0 & w_{2,3} & w_{2,4} & w_{2,5} & w_{2,6} & w_{2,7} & w_{2,8} & 0 & 0 \\ 0 & 0 & 0 & 0 & 0 & 0 & w_{3,7} & w_{3,8} & w_{3,9} & w_{3,10} \end{pmatrix}. \tag{18}$$

The moment-arms created by muscles $\mathscr{M}_5$, $\mathscr{M}_6$, $\mathscr{M}_7$ and $\mathscr{M}_8$ around the first joint and the moment-arms created by muscles $\mathscr{M}_9$ and $\mathscr{M}_{10}$ around the second joint are set to zero. These coupling terms are the moment-arms created by the muscles which do not span the joints, but still create moment-arms at these joints. The mechanical equilibrium is solved using both moment-arm matrices (14) and (18).

Once a solution to the problem is found, the reaction forces in the three joints are computed using Newton's second law of motion applied to each body:

$$\mathbf{f}_{\mathrm{react},J_3} = m_3\mathbf{a}_3 - \mathbf{f}_{\mathrm{muscle},\mathscr{B}_3} + m_3\mathbf{g}, \tag{19}$$

$$\mathbf{f}_{\mathrm{react},J_2} = m_2\mathbf{a}_2 - \mathbf{f}_{\mathrm{muscle},\mathscr{B}_2} + m_2\mathbf{g} + \mathbf{f}_{\mathrm{react},J_3}, \tag{20}$$

$$\mathbf{f}_{\mathrm{react},J_1} = m_1\mathbf{a}_1 - \mathbf{f}_{\mathrm{muscle},\mathscr{B}_1} + m_1\mathbf{g} + \mathbf{f}_{\mathrm{react},J_2}. \tag{21}$$

Vectors $\mathbf{a}_i$ are the accelerations of the centres of gravity of each body. Vectors $\mathbf{f}_{\mathrm{muscle},\mathscr{B}_i}$ are the muscle forces applied to body $\mathscr{B}_i$.

2.3 *Null-space optimisation*

In the context of muscle-force estimation, the solution to the optimisation problem is not defined by the cost function but rather by constraints (16) and (17). Indeed, the cost function simply represents a means of choosing a

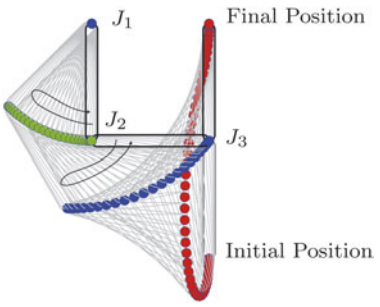

Figure 6. Stroboscopic diagram of the motion used to carry out the estimations.

solution. And the set of all feasible solutions is defined by the torque–force relation (16), while the second constraint (17) limits the search to a subset. Thus, relation (16) can be directly used to parameterise solution $\mathbf{f}_k$:

$$\mathbf{f}_k = \mathbf{f}_{0k} + \mathbf{N}_k \mathbf{v}_k. \tag{22}$$

This relation expresses the solution as an initial solution $\mathbf{f}_{0k}$, which respects relation (16), and a correction term parameterised by a vector $\mathbf{v}_k$. Matrix $\mathbf{N}_k$ is the null-space matrix of the moment-arm matrix. The correction vector $\mathbf{v}_k$ is projected onto the null-space of the moment-arm matrix, such that one can search for a solution, which respects the second set of constraints, but does not violate the torque–force constraint. The re-parameterisation of the optimisation problem in terms of (22) is defined by the following quadratic program:

$$\min \quad g(\mathbf{v}_k) = \frac{1}{2}\mathbf{v}_k^{\mathrm{T}}\mathbf{H}\mathbf{v}_k + \mathbf{h}\mathbf{v}_k, \tag{23}$$

$$\text{s.t.} \quad \mathbf{A}\mathbf{v}_k - \mathbf{b} \leq 0, \quad \min/\max \text{ force}. \tag{24}$$

A detailed presentation of this re-parameterisation is given in Aeberhard et al. (2009) and Terrier et al. (2010).

2.4 *Movement*

The planned motion is defined by the following set of expressions (Figure 6):

$$\begin{aligned} \theta_1 &= -\frac{\pi}{8}\left(1 - \cos\left(2\pi\frac{t}{T}\right)\right), \\ \theta_2 &= -\frac{\pi}{6}\left(1 - \cos\left(2\pi\frac{t}{T}\right)\right), \\ \theta_3 &= \frac{\pi}{2}\left(1 - \cos\left(2\pi\frac{t}{T}\right)\right). \end{aligned} \tag{25}$$

The muscle forces are estimated for a dynamic motion, with $T = 1$ s, and the reaction forces in the three joints are computed.

3. Results

Using the two moment-arm matrices (10) and (14) yielded two very distinct behaviours. The estimated muscle forces are presented for each muscle (Figure 7). The difference was 100% for muscles $\mathscr{M}_1$, $\mathscr{M}_2$, $\mathscr{M}_5$ and $\mathscr{M}_{10}$. Muscles $\mathscr{M}_5$ and $\mathscr{M}_{10}$ were active using the incorrect definition, while using the correct definition $\mathscr{M}_{10}$ was not active and $\mathscr{M}_5$ was only slightly active. Certain muscles ($\mathscr{M}_3$, $\mathscr{M}_7$ and $\mathscr{M}_8$) had short periods in which the two behaviours coincided but were dissimilar otherwise.

The amplitude of the reaction forces in the three joints is presented for the entire motion (Figure 8(a)). The moment-arm matrices (10) and (14) also modified the joint reaction forces which had the same range of amplitude.

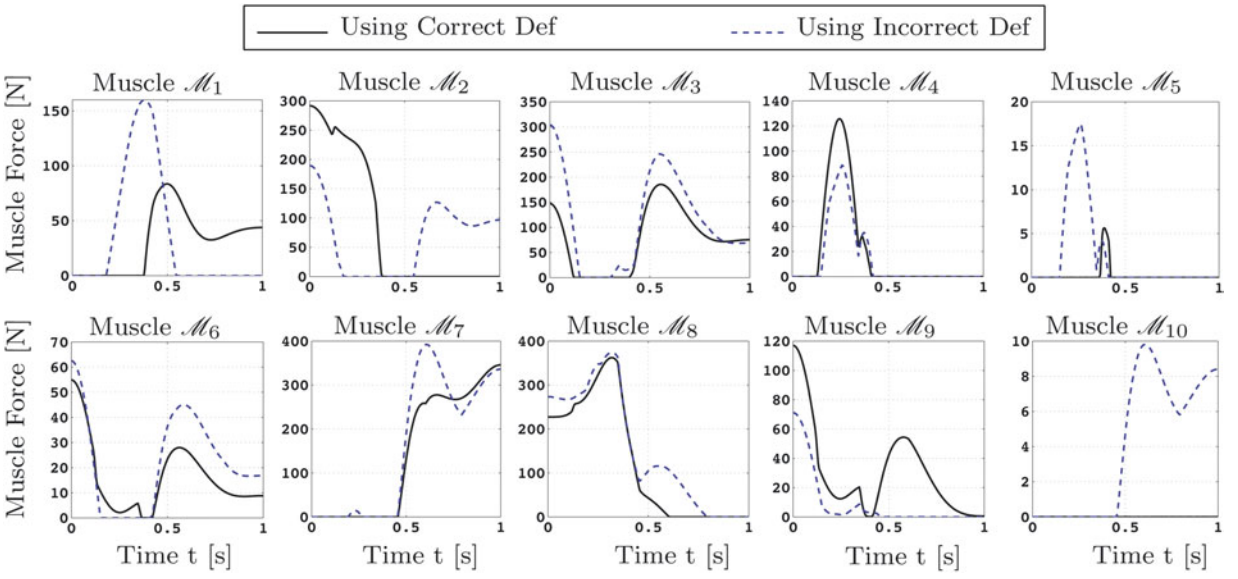

Figure 7. Estimated muscle forces for the different muscles using both the correct and incorrect moment-arm definitions.

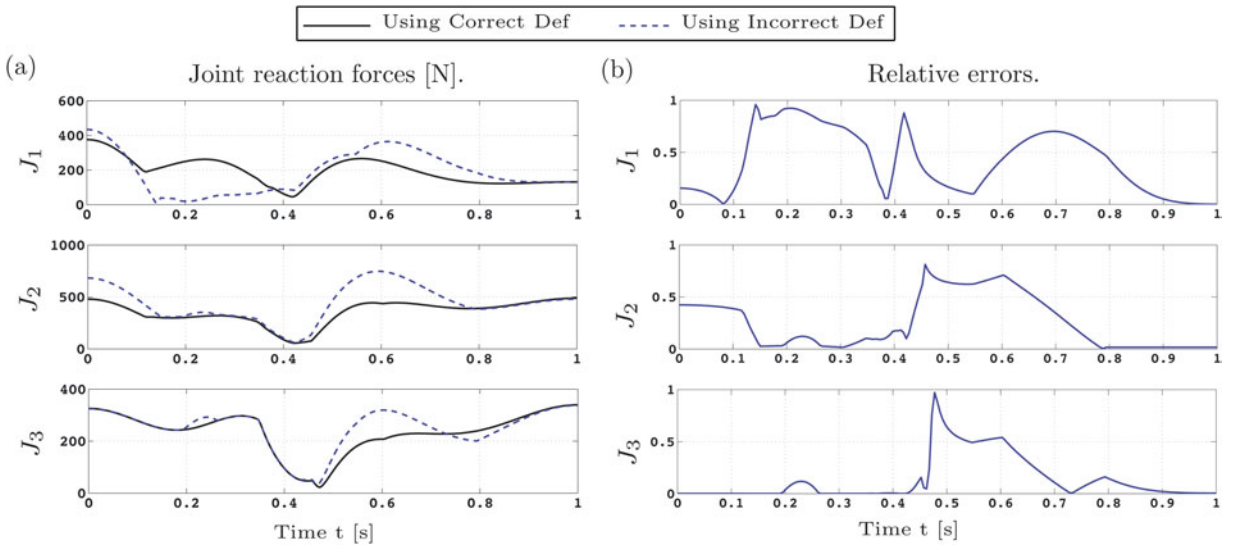

Figure 8. Comparison of the reaction forces (N) in the joints (a) using the correct and incorrect moment-arm definitions during the entire motion and relative errors between the joint reaction forces (b) obtained using the correct and incorrect moment-arm definitions.

The relative errors between the two solutions varied between 0% and almost 100% (Figure 8(b)). The reaction force in the third joint has the least error and the reaction force in the first joint has the most error.

4. Discussion

In the introduction, it was stated that the tendon excursion method is defined using an analytical mechanics framework and therefore requires the same level of detail. A number of examples from the literature used tendon-excursion method without the necessary rigorous justification (Herzog and Binding 1992; Raikova and Prilutsky 2001; Menegaldo et al. 2004; Rankin and Neptune 2012), which has led to an incorrect definition that muscles only generate moment-arms at the joints spanned by the muscle. The main weakness of the tendon excursion method is its dependency on the choice of joint coordinates. Therefore, the goal of this paper was to present a clear and unambiguous definition of muscle moment-arms. The definition presented is constructed using screw theory and classical mechanics, leading to a geometric definition of muscle moment-arms independent of the coordinates used to describe the system. The magnitude of the error made by an inappropriate application of the tendon excursion method was assessed by comparing the solutions of a muscle-force estimation problem for a conceptual 2D musculoskeletal model.

The definition of moment-arms and the proposed construction method presented in this paper apply to musculoskeletal models in which the bones are modelled as rigid bodies, the joints are modelled as ideal mechanical joints and the muscles are modelled as massless, frictionless cables wrapping over bony protrusions, approximated using geometric surfaces. The model is governed by classical mechanics, by which the system is defined by the bones and joints, while the muscles act as external force generators, and can be treaded using pulley mechanics. In this context, the proposed definition of moment-arm is complete in a mechanical sense and the method of computation is exact with respect to the geometry of the model.

The error made from applying the tendon excursion method without the necessary rigour stems from the location where the muscles create moment-arms. If applied inappropriately, the method yields moment-arms only at the joints spanned by the muscles. In contrast, the definition presented in this paper yields moment-arms at the joints spanned by the muscles *and* at the neighbouring joints attached to the bodies on which the muscles insert and originate. Confirmation of this definition was obtained using the tendon excursion method with absolute coordinates to compute the moment-arms. An example was given where identical moment-arms were obtained at the joints spanned by the muscles and the joints not spanned by the muscles.

The moment-arms at the joints not spanned by the muscle create a coupling effect. The muscle-force prediction was substantially different when coupling moment-arms were not included. The reason for this difference is that omitting the coupling terms relaxes the optimisation problem independent of the cost function. For instance, the two muscles $\mathscr{M}_9$ and $\mathscr{M}_{10}$ are activated to generate the necessary torque around the third joint. In doing so, a torque is also generated at the second joint not spanned by the muscles. This torque must be compensated for by the muscles directly affecting this joint such as $\mathscr{M}_5$ and $\mathscr{M}_6$. However, these muscles must also create the required torque to generate the motion. The coupling effect can be beneficial by reducing the load on the other muscles or detrimental, making them reach their maximum force quicker. In the 2D setting, this coupling

effect has little impact on the system's ability to generate torque around the joint. However, in a 3D setting, this effect can lead to the estimation problem being infeasible, a problem observed in Ingram et al. (2012).

As stated previously, the effect of the coupling terms is independent of the cost function and the method used to resolve the optimisation problem. The null-space method was used both because it has shown promising results (Aeberhard et al. 2009; Terrier et al. 2010) and because it helped to pinpoint the nature of the unfeasibility observed in Ingram et al. (2012) due to its direct use of the map (13) to construct the solution.

The theoretical problem presented in this paper highlights the importance of a correct calculation of moment-arms when using optimisation techniques to estimate muscle forces. In order for the optimisation problem to have a solution, the imposed moment of force must be in the range space of the moment of force/muscle-force map (13). This remark underlines the essential role played by the moment-arms, which define this range space.

Acknowledgement

This study was supported by the Swiss National Science Foundation (No. K-32K1_122512).

Notes

1. Email: david.ingram@epfl.ch
2. Email: christoph.engelhardt@epfl.ch
3. Email: alexander.terrier@epfl.ch
4. Notation: bold lower-case letters are vectors, bold upper-case letters are matrices, plain lower-case letters are scalars and plain upper-case letters are geometric points.

References

Ackland D, Pak P, Richardson M, Pandy M. 2008. Moment arms of the muscles crossing the anatomical shoulder. J Anat. 213 (4):383–390.

Aeberhard M, Michellod Y, Mullhaupt P, Terrier A, Pioletti D, Gillet D. 2009. Dynamical biomechanical model of the shoulder: null space based optimization of the overactuated system. In: IEEE International Conference on Robotics and Biomimetics; 2008 Feb 21–26; Bankok, Thailand. ROBIO 2008; February. p. 67–73.

An K, Takahashi K, Harrigan T, Chao E. 1984. Determination of muscle orientations and moment arms. J Biomech Eng. 106 (3):280–282.

An K, Ueba Y, Chao E, Cooney W, Linscheid R. 1983. Tendon excursion and moment arm of index finger muscles. J Biomech. 16(6):419–425.

Ball SR. 1876. Theory of screws: a study in the dynamics of a rigid body. Dublin: Hodges Publication.

Brand PW, Cantor KC, Ellis JC. 1975. Tendon and pulleys at the metacarpophalangeal joint of a finger. J Bone Joint Surg. 57 (6):779–784.

Charlton W, Johnson G. 2001. Application of spherical and cylindrical wrapping algorithms in a musculoskeletal model of the upper limb. J Biomech. 34(9):1209–1216.

Garner B, Pandy M. 1999. Musculoskeletal model of the upper limb based on the visible human male dataset. Comput Methods Biomech Biomed Eng. 4(2):107–124.

Garner B, Pandy M. 2001. A kinematic model of the upper limb based on the visible human project (VHP) image dataset. Comput Methods Biomech Biomed Eng. 2(2):93–126.

Gruber C, Benoit W. 1998. Méchanique Générale. Lausanne: Presses Polytechniques et Universitaires Romandes.

Happee R. 1994. Inverse dynamic optimization including muscular dynamics, a new simulation method applied to goal directed movements. J Biomech. 27(7):953–960.

Herzog W, Binding P. 1992. Predictions of antagonistic muscular activity using nonlinear optimization. Math Biosci. 111 (2):217–229.

Holzbaur K, Murray WM, Delp S. 2005. A model of the upper extremity for simulating musculoskeletal surgery and analyzing neuromuscular control. Ann Biomed Eng. 33:829–840.

Ingram D, Muellhaupt P, Terrier A, Pralong E, Farron A. 2012. Dynamical biomechanical model of the shoulder for muscle-force estimation. In: 2012 4th IEEE RAS & EMBS International Conference on Biomedical Robotics and Biomechatronics (BioRob); 2012 June 24–27; Rome. p. 407–412.

Liu J, Hughes R, Smutz W, Niebur G, Nan-An K. 1997. Roles of deltoid and rotator cuff muscles in shoulder elevation. Clin Biomech. 12(1):32–38.

Menegaldo L, deToledo Fleury A, Weber H. 2004. Moment arms and musculotendon lengths estimation for a three-dimensional lower-limb model. J Biomech. 37(9):1447–1453.

Otis J, Jiang CC, Wickiewicz T, Peterson M, Warren R, Santner T. 1994. Changes in the moment arms of the rotator cuff and deltoid muscles with abduction and rotation. J Bone Joint Surg. 76(5):667–676.

Raikova R, Prilutsky B. 2001. Sensitivity of predicted muscle forces to parameters of the optimization-based human leg model revealed by analytical and numerical analyses. J Biomech. 34(10):1243–1255.

Rankin J, Neptune R. 2012. Musculotendon lengths and moment arms for a three-dimensional upper-extremity model. J Biomech. 45(9):1739–1744.

Terrier A, Aeberhard M, Michellod Y, Mullhaupt P, Gillet D, Farron A, Pioletti D. 2010. A musculoskeletal shoulder model based on pseudo-inverse and null-space optimization. Med Eng Phys. 32(9):1050–1056.

Whittaker T. 1927. A treatise on the analytical dynamics of particles and rigid bodies. Analytical dynamics. 3rd ed.. Cambridge: Cambridge University Press.

Yeung S. 1995. The triple spherical pendulum. California Institute of Technology, Division of Chemistry and Chemical Engineering. Technical report.